IEEE Access
Multidisciplinary ⋮ Rapid Review ⋮ Open Access Journal

Received 5 March 2024, accepted 30 March 2024, date of publication 4 April 2024, date of current version 22 April 2024.

Digital Object Identifier 10.1109/ACCESS.2024.3384564

RESEARCH ARTICLE

Computationally Efficient Reduced Order Modeling of DFIG-Based Wind Turbines: A Novel Frequency-Weighted and Limited Model Reduction Approach With Error Bounds

MUHAMMAD LATIF[1], HIRA AMBREEN[2], FARRUKH HASSAN[3], (Graduate Student Member, IEEE), MUHAMMAD IMRAN[1], AND MUHAMMAD IMRAN[1]

[1]Department of Electrical Engineering, Military College of Signals (MCS), National University of Sciences and Technology (NUST), Islamabad 43000, Pakistan
[2]Department of Electrical Engineering, Sir Syed Center for Advanced Studies in Engineering Institute of Technology (SS-CASE-IT), Islamabad 43000, Pakistan
[3]Department of Computing and Information Systems, School of Engineering and Technology, Sunway University, Bandar Sunway, Subang Jaya 47500, Malaysia

Corresponding author: Muhammad Imran (muhammad.imran79@ee.ceme.edu.pk)

ABSTRACT In wind turbine engineering, stability and control rely on precision. A new approach for discrete-time systems is presented in this study, which makes use of constrained Gramians and frequency weights. Wind turbines with a double-fed induction generator and dynamic rotational speeds can have their model order reduced using the suggested method, which makes use of sophisticated state-space representations. A novel balanced realization method, along with frequency-weighted and limited Gramians, successfully lowers the dimensionality of large state models. Minimizing approximation errors and ensuring stability are both achieved by the resulting lower-order system. This paper makes a significant contribution by offering an *a priori* formula for error boundaries, which allows for more efficient and faster computations. A paradigm shift in improving the accuracy of modeling techniques is marked by this groundbreaking method, which applies frequency-weighted and limited Gramians to real-time systems like wind turbines.

INDEX TERMS Frequency weighted Gramians, frequency limited Gramians, balance algorithm, model reduction, error-bound, induction generator, wind turbine.

ABBREVIATIONS AND ELEMENTARY OPERATORS

Table 1 briefly summarize some abbreviations and elementary operators with their terminologies.

I. INTRODUCTION

Improving turbine technology is driven by the primary quest of efficiently generating electrical power using the wind's kinetic energy [1], [2], [3], [4], [5]. Notable machines in this category include Permanent Magnet Synchronous Generators (PMSGs), Double-Fed Induction Generators (DFIGs), and Squirrel Cage Induction Generators (SCIGs) [6], [7]. In particular, DFIGs resist grid ride-through issues with high and low voltages [8], which solidifies their importance in wind energy conversion systems [9]. Their versatility, manageability, remarkable energy efficiency, better power quality, and other outstanding qualities lead to their extensive use [9].

The addition of reactive power compensators enhances the complexity of wind energy conversion systems, which

The associate editor coordinating the review of this manuscript and approving it for publication was Bidyadhar Subudhi.

TABLE 1. Abbreviations and elementary operators.

Abbreviation	Full Form	Elementary Operator	Terminology
PMSG	Permanent Magnet Synchronous Generator	H	Inertia constant of load and rotor
DFIG	Double-Fed Induction Generator	F	Viscous friction of load and rotor
SCIG	Squirrel Cage Induction Generator	ω_m	Angular velocity of rotor
DCIM	Double Cage Induction Machine	T_e	Torque based on electromagnetism
SCIM	Squirrel Cage Induction Machine	T_m	Torque based on mechanical shaft
LVRT	Low Voltage Ride Through	L_m	Magnetic-Inductance
HVRT	High Voltage Ride Through	p	Number of Pole-Pairs
WT	Wind Turbine	$H[z]$ and $H_{tr}[z]$	Original and reduced systems's transfer function
ROM	Reduced-Order Model	P_{BT} and Q_{BT}	Original systems's Gramians matrices
MOR	Model Order Reduction	$V_{iw}[z]$ and $W_{ow}[z]$	Input and output weighted systems's transfer function
BT	Balanced Truncation	T_f	Transformation matrix
WZ	Wang & Zilouchian	ψ_i	Sigma values for $i = 1, 2, 3, \ldots, n$
CB	Campbell	X_E and Y_E	Input and output associated matrices
GS	Ghafoor & Sreeram	$\leq$	Less than or equal to
SI	Sammana & Imran	$\geq$	Greater than or equal to
IG	Imran & Ghafoor	$\in$	Belongs to
TI	Toor & Imran	$\|\|(.)\|\|_\infty$	Infinity norm
HSV	Hankel Singular Values	$\sum_{n_1}^{n_2}$	Discrete sum

include double cage induction machines (DCIMs) and single cage induction machines (SCIMs) [10], [11]. When using a SCIM with two squirrel cages instead of one with one cage, the order and complexity increase exponentially. Strict adherence to grid standards is necessary to reduce power outages because of the constantly changing wind conditions, which impact density, velocity, and temperature [8], [11]. The integration of wind farms with the grid is further complicated by diverse grid codes designed to meet each country's specific operating requirements and environmental conditions of each country [12], [13].

The following features are covered in this work: controls (active/reactive power, external and communications, voltage and frequency control), operational ranges (frequency and voltage), ride-through capabilities (low voltage ride-through (LVRT) and high voltage ride-through (HVRT)), wind farm verification and modeling for improved accuracy and reliability, and power quality improvement. For effective study, energy systems, such as wind turbines (WTs), require reduced-order models (ROMs) [14]. By utilizing Gramians-based balanced realization, ROM state-space representations substantially contribute to WT stability, controllability, and observability investigations. Researchers and practitioners can better understand energy systems, especially WTs, with the help of the following ROMs.

The simplification of analysis, design, and simulation of higher-order systems is greatly aided by model order reduction (MOR), which is commonly achieved through balanced truncation (BT) [15] in the field of control theory [16], [17], [18]. Adaptations such as the frequency-weighted (i.e., Enns approach) and restricted-frequency interval (i.e., Wang & Zilouchian (WZ)) techniques have been implemented because some shortcomings of BT still exist, even though it has been widely used [19], [20], [21]. However, these methodologies [19], [21] also have some drawbacks,such as instability and loss of minimality. Many attempts were made by the researchers to address this significant drawback, based on frequency-weighted [22], [23], [24] (i.e., Campbell (CB) [22], Ghafoor & Sreeram (GS) [23] and Sammana & Imran (SI) [24]) and frequency-limited interval (i.e., Imran & Ghafoor (IG) [25], Toor & Imran (TI) [26] and Sammana & Imran (SI) [24]) MOR approaches.

A critical research need will be satisfied by overcoming the significant disparities between the input and output matrices, which lead to approximation errors and instability issues in ROMs. The main reason why the current methods frequently deviate from ROMs and the original dynamics of the system is that they handle the input and output matrices incorrectly. These variances lower the accuracy and dependability of ROMs by raising the possibility of instability and producing large approximation mistakes. By developing a novel MOR technique that blends frequency-weighted truncation with limited interval balanced truncation, our work seeks to close this gap [19], [21].

Based on stability-preserving MOR, the proposed method yields a computable *a priori* error-bound expression for variable-speed WTs [27]. It is possible to achieve stability and reduced approximation error by carefully improving the input and output matrices. As a result, authority is distributed fairly in light of the system's distinctive tenets. Unlike traditional approaches, our system aggressively guarantees that energy is dispersed uniformly among related states, thereby collectively normalising the impact of improvements on the matrices corresponding to the input and output. We have confirmed via extensive simulations that our proposed approach is more realistic and effective than the current ones. The comparison's outcomes, the simulation method, MOR's theoretical foundations, comparison results, simulation methodology, and its application to wind farms. Finally, we provide a brief overview of our findings and suggest areas for further research.

II. GRID INTERFACES FOR INDUCTION MACHINES

A. DFIG GRID INTERFACE ARRANGEMENT

A gearbox increases the rotating speed of the shaft that connects the DFIG rotor to the WT, as shown in Figure 1, allowing for grid connectivity for DFIGs. The wound rotor can be connected to the grid with the help of two AC-DC-AC converters, which guarantee conversion of approximately 30 percent of the total power production. The DC-link capacitor is used to store the generated power. Regardless of variations in wind speed, the DFIG uses converters to keep the output frequency constant by grid requirements. Intricate control systems regulate input, reactive power, and grid terminal voltage; a step-up transformer links the DFIG's stator to the power grid. Using our all-encompassing control system, wind power can be reliably generated [28], [29].

Remark 1: Sophisticated control algorithms are needed to guarantee the reliable and effective operation of DFIG systems, especially when handling variable wind conditions. It could be difficult to achieve optimal control performance while taking uncertainties and system limitations into account.

Remark 2: Reactive power support and fault ride-through capabilities are two grid code requirements that must be addressed in order to integrate DFIG systems with the electrical grid. Maintaining grid stability requires smooth and dependable grid integration, but this comes with a lot of challenging technological issues.

B. SCIG GRID INTERFACE ARRANGEMENT

The power grid is always linked to wind turbines, regardless of whether they are double- or single-cage SCIGs with set rotational speeds [30]. A simplified representation of the system is shown in Figure 2, which emphasizes the power factor enhancement by employing capacitor banks and reactive power compensators. Maximizing wind generation while reducing the effect of wind fluctuations on the rotor's rotational speed is achieved by rotor pitch angle adjustment. All the parts of WTs that depend on different speeds are contained in the metaphorical "squirrel cages.".

III. DCIM: A MATHEMATICAL MODEL

The mathematical relations used to harvest wind energy are listed in [31], [32], and [33]. The mathematical model represents every electrical variable and stator property as an integer. Table 2 lists the different DCIM options.

A. MATHEMATICAL FORM OF AN ELECTRICAL MODEL

The electrical arrangement includes several brushes, along with a stator and two squirrel cages. The mechanical part is detailed extensively in the first situation, whereas in the second case, the entire process is elucidated [34]. Figure 3 shows the circuit simplified. The stator voltages (d) and (q) can be determined using the computations given below (refer to Table 3):

$$V_{q_s} = R_s i_{q_s} + \frac{d\varphi_{q_s}}{dt} + \omega\varphi_{d_s},$$
$$V_{d_s} = R_s i_{d_s} + \frac{d\varphi_{d_s}}{dt} - \omega\varphi_{q_s}.$$

For the first cage, we have the following equations for the q- and d-axis rotors:

$$0 = \acute{R}_{r_1}\acute{i}_{q_{r_1}} + \frac{d\acute{\varphi}_{q_{r_1}}}{dt} + (\omega - \omega_r)\acute{\varphi}_{d_{r_1}},$$
$$0 = \acute{R}_{r_1}\acute{i}_{d_{r_1}} + \frac{d\varphi_{d_{r_1}}}{dt} + (\omega - \omega_r)\acute{\varphi}_{q_{r_1}}.$$

Similarly, for the second cage, we have the following equations for the q- and d-axis rotors:

$$0 = \acute{R}_{r_2}\acute{i}_{q_{r_2}} + \frac{d\acute{\varphi}_{q_{r_2}}}{dt} + (\omega - \omega_r)\acute{\varphi}_{d_{r_2}}$$
$$0 = \acute{R}_{r_2}\acute{i}_{d_{r_2}} + \frac{d\varphi_{d_{r_2}}}{dt} + (\omega - \omega_r)\acute{\varphi}_{q_{r_2}}$$

Dual squirrel-cage induction motors' behaviour can be modelled with an electrical torque equation, as shown below:

$$T_e = 1.5p(\omega\varphi_{d_s} i_{q_s} - \omega\varphi_{q_s} i_{d_s})$$

Remark 3: Dynamic responses to wind speed variations, grid outages, and control commands are demonstrated by DFIG systems. It is necessary to regulate transient behaviours like voltage deviations and rotor speed fluctuations in order to maintain system stability and performance.

Remark 4: In order to ensure that DFIG systems operate as consistently and efficiently as is reasonably possible, ongoing maintenance is required. It can be challenging to locate and diagnose defects like converter failures and bearing wear, particularly in remote offshore areas.

Remark 5: It is difficult to strike a compromise between component part costs and the performance and efficiency requirements of the DFIG system. For DFIG system developers, meeting efficiency standards and creating efficient systems with low setup and operating costs continue to be important goals.

B. MATHEMATICAL FORM OF A MECHANICAL MODEL

The mechanical system of the DCIM at the second-order level is depicted in this picture [27]:

$$\frac{d}{dt}\omega_m = \frac{1}{2H}(T_e - F\omega_m - T_m)$$

where $\omega_m = \frac{d}{dt}\theta_m$.

IV. BALANCED TRUNCATION TECHNIQUE

Here, we have a discrete linear time-invariant (LTI) system characterized by the following equations:

$$\dot{x}[k] = Ax[k] + Bu[k],$$
$$y[k] = Cx[k] + Du[k],$$
$$H[z] = C[zI - A]^{-1}B + D, \quad (1)$$

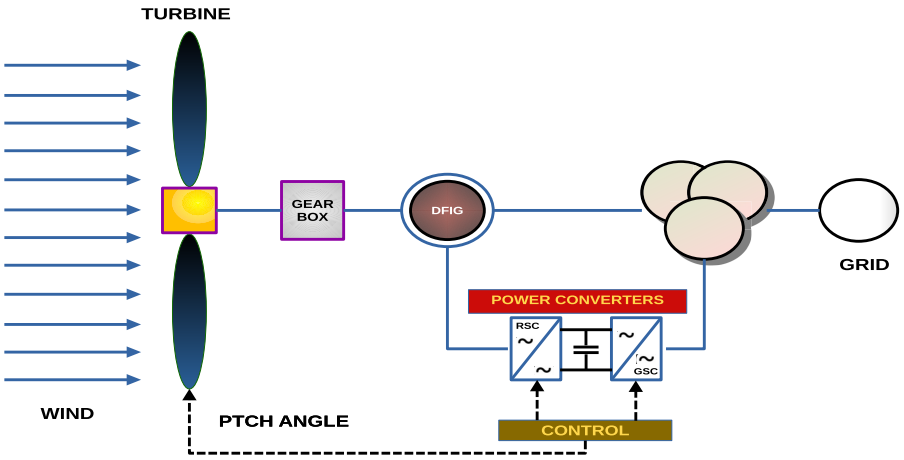

FIGURE 1. Simplified DFIG grid integration.

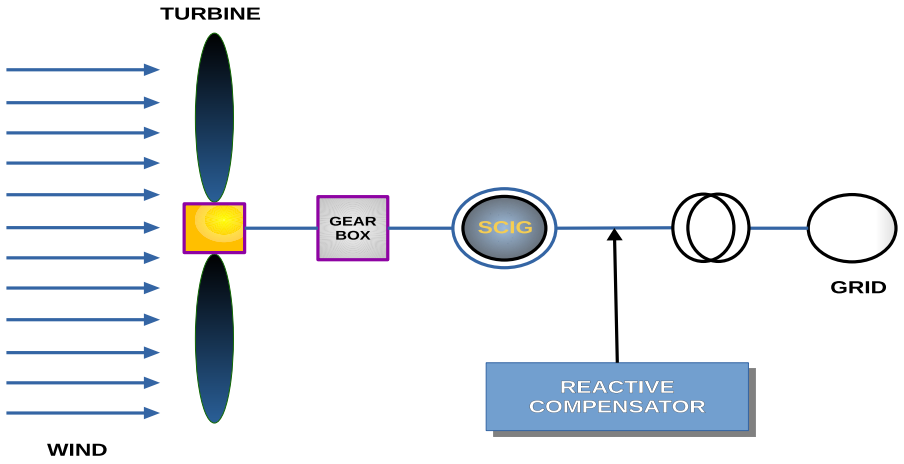

FIGURE 2. Simplified SCIG grid integration.

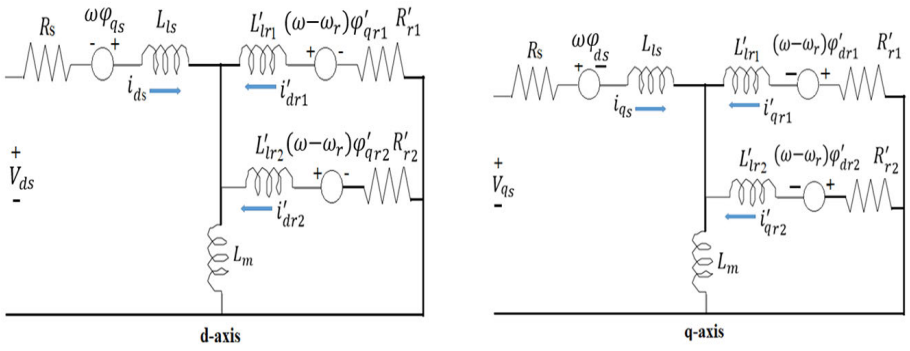

FIGURE 3. A DCIM's electrical circuit in the dq- or dual-axis frame of reference system.

where $A \in \Re^{n\times n}$, $B \in \Re^{n\times p}$, $C \in \Re^{q\times n}$, and $D \in \Re^{q\times p}$ form a minimal and stable discrete-time realization with p inputs and q outputs. The goal of MOR is to obtain a reduced-order mathematical model for discrete-time systems.

Similarly, the reduced-order system is given by:

$$\begin{aligned} \dot{x}_{tr}[k] &= A_{tr}x_{tr}[k] + B_{tr}u[k], \\ y[k] &= C_{tr}x_{tr}[k] + D_{tr}u[k], \\ H_{tr}[z] &= C_{tr}[zI - A_{tr}]^{-1}B_{tr} + D_{tr}, \end{aligned} \tag{2}$$

TABLE 2. Options for DCIM.

Option	Description
Option 1	Makes use of a three-phase stator arrangement fine-tuned for maximum efficiency under light wind circumstances. Incorporating meticulously planned winding patterns and the dispersion of magnetic fields, this option improves performance even when wind speeds are less than ideal. The stator design uses modern materials to reduce losses and increase power output.
Option 2	Improves longevity and cuts down on maintenance needs using modern brush materials and designs. The brushes are designed to endure severe weather, lasting longer and working reliably even in the most difficult environments. This choice makes the power transfer between the revolving and stationary parts efficient, and the electrical contact is stable.
Option 3	It reaches peak performance and stability across a broad speed range, even in high-wind conditions, thanks to a rotor design that uses two squirrel cages. Careful consideration of the wind conditions at the time of rotor design is essential for achieving peak performance. We can try to comprehend the overall effect of the rotor cages on system behavior by adding dual rotor dynamics to the mathematical model.
Option 4	One distinctive feature of the DCIM design is the built-in electromagnetic braking mechanism. This option offers efficient braking systems to keep you safe and in control of windy conditions, reducing the likelihood of damage and overspeeding. Incorporating electromagnetic brake dynamics equations into the mathematical model allows for a realistic depiction of the braking system's effect on DCIM performance.

TABLE 3. The DCIM's parameters.

Parameters for the DCIM			
Stator of the DCIM		**Dual-Cage Rotor of the DCIM**	
R_s, L_{l_s}	Stator-Resistance, Leakage-Inductance	$\acute{R}_{r_1}, \acute{L}_{l_{r_1}}$	Rotor-Resistance, and Inductance-Leakage in cage 1
L_s	Stator-Inductance	$\acute{R}_{r_2}, \acute{L}_{l_{r_2}}$	Rotor-Resistance, Leakage-Inductance in the cage-2
V_{q_s}, i_{q_s}	Stator-Voltage, Stator-Current in q-axis	$\acute{L}_{r_1}, \acute{L}_{r_2}$	Rotor-Inductances in cages 1 and 2
V_{d_s}, i_{d_s}	Stator-Voltage, Stator-Current in d-axis	$\acute{i}_{d_{r_1}}, \acute{i}_{d_{r_2}}$	Rotor-Current in cages 1 and 2 along the d-axis
φ_{d_s}	Stator-Flux in d-axis	$\acute{i}_{q_{r_1}}, \acute{i}_{q_{r_2}}$	Rotor-Current in cages 1 and 2 along the q-axis
φ_{q_s}	Stator-Fluxes in q-axis	$\acute{\varphi}_{d_{r_1}}, \acute{\varphi}_{q_{r_1}}$	Rotor-Fluxes in cage 1 along the dq-axis
$\acute{\varphi}_{d_{r_2}}, \acute{\varphi}_{q_{r_2}}$	Rotor-Fluxes in cage 2 along the dq-axis		

where $A_{tr} \in \Re^{r\times r}$, $B_{tr} \in \Re^{r\times p}$, $C_{tr} \in \Re^{q\times r}$, and $D_{tr} \in \Re^{q\times p}$ constitute the reduced-order discrete-time realization with $r \ll n$.

The Gramians for entire-frequency controllability (i.e., P_{BT}) and entire-frequency observability (i.e., Q_{BT}) are defined as [15]:

$$P_{BT} = \frac{1}{2\pi}\int_{-\pi}^{\pi}[e^{j\omega}I - A]^{-1}BB^T[e^{-j\omega}I - A^T]^{-1}d\omega,$$
$$Q_{BT} = \frac{1}{2\pi}\int_{-\pi}^{\pi}[e^{-j\omega}I - A^T]^{-1}C^TC[e^{j\omega}I - A]^{-1}d\omega,$$

These Gramians satisfy the following Lyapunov equations:

$$APA^T - P + BB^T = 0,$$
$$A^TQA - Q + C^TC = 0.$$

To achieve a balanced realization, a transformation matrix T_f is constructed such that:

$$T_f^TQT_f = T_f^{-1}PT_f^{-T} = diag\{\psi_1, \psi_2, \psi_3, \ldots, \psi_n\}, \quad (3)$$

where $\psi_i \geq \psi_{i+1}$ for $i = 1, 2, 3, \ldots, n-1$, and $\psi_r > \psi_{r+1}$.

The realized model is then partitioned into ROMs:

$$T_f^{-1}AT_f = \begin{bmatrix} A_r & A_{12} \\ A_{21} & A_{22} \end{bmatrix}, \quad T_f^{-1}B = \begin{bmatrix} B_r \\ B_2 \end{bmatrix} \quad (4)$$
$$CT_f = \begin{bmatrix} C_r & C_2 \end{bmatrix}, \quad D = D_r. \quad (5)$$

Remark 6: The associated ROMs $\{A_r, B_r, C_r\}$ maintain the stability and minimality of a discrete-time realization $\{A, B, C\}$ [15]. The choice of $\{T_f^{-1}AT_f, T_f^{-1}B, CT_f\}$ also determines the frequency response error bounds for the balancing realization with the parameter settings.

Remark 7: Particularly, the balancing transformation T_f lines up the system's modes so that the ROM captures the most important dynamics, guaranteeing a successful decrease in computing complexity without sacrificing fundamental system behaviors [15].

Remark 8: The resultant diagonal matrix's diagonal elements represent the system's singular values; these values shed light on how each mode contributes to the system's overall behavior [15].

A. WEIGHTED MOR PROBLEM

1) AUGMENTED REALIZATIONS

Here, we have an input-weighting discrete LTI system characterized by the following equations:

$$\dot{x}_{iw}[k] = A_{iw}x_{iw}[k] + B_{iw}u_{iw}[k],$$
$$y_{iw}[k] = C_{iw}x_{iw}[k] + D_{iw}u_{iw}[k],$$
$$V_{iw}[z] = C_{iw}[zI - A_{iw}]^{-1}B_{iw} + D_{iw}, \quad (6)$$

Here, $\{A_{iw}, B_{iw}, C_{iw}, D_{iw}\}$ denote the $n_{iw}{}^{th}$ order input-weighting minimal and stable realization, where $A_{iw} \in \Re^{n_{iw}\times n_{iw}}$, $B_{iw} \in \Re^{n_{iw}\times m_{iw}}$, $C_{iw} \in \Re^{p_{iw}\times n_{iw}}$, $D_{iw} \in \Re^{p_{iw}\times m_{iw}}$, n_{iw}, m_{iw}, and p_{iw} represent the order of the input-weighting, the total number of inputs, and the total number of outputs, respectively.

Similarly, we have a discrete LTI output-weighting system described by the following equations:

$$\dot{x}_{ow}[k] = A_{ow}x_{ow}[k] + B_{ow}u_{ow}[k],$$
$$y_{ow}[k] = C_{ow}x_{ow}[k] + D_{ow}u_{ow}[k],$$

$$W_{ow}[z] = C_{ow}[zI - A_{ow}]^{-1}B_{ow} + D_{ow}, \tag{7}$$

Here, $\{A_{ow}, B_{ow}, C_{ow}, D_{ow}\}$ denote the $n_{ow}{}^{th}$ order output-weighting stable and minimal realization, where $A_{ow} \in \Re^{n_{ow}\times n_{ow}}$, $B_{ow} \in \Re^{n_{ow}\times m_{ow}}$, $C_{ow} \in \Re^{p_{ow}\times n_{ow}}$, $D_{ow} \in \Re^{p_{ow}\times m_{ow}}$. In this case, n_{ow}, m_{ow}, and p_{ow} are the order of output-weighting realization, the number of inputs, and the number of outputs, respectively.

The weighted input-augmented and weighted output-augmented systems $H[z]V_{iw}[z]$ (i.e., $\{A_{ia}, B_{ia}, C_{ia}, D_{ia}\}$) and $W_{ow}[z]H[z]$ (i.e., $\{A_{oa}, B_{oa}, C_{oa}, D_{oa}\}$), respectively, are given by:

$$H[z]V_{iw}[z] = C_{ia}[zI - A_{ia}]^{-1}B_{ia} + D_{ia},$$
$$W_{ow}[z]H[z] = C_{oa}[zI - A_{oa}]^{-1}B_{oa} + D_{oa},$$

where

$$\left[\begin{array}{c|c} A_{ia} & B_{ia} \\ \hline C_{ia} & D_{ia} \end{array}\right] = \left[\begin{array}{cc|c} A & BC_{iw} & BD_{iw} \\ 0 & A_{iw} & B_{iw} \\ \hline C & DC_{iw} & DD_{iw} \end{array}\right],$$
$$\left[\begin{array}{c|c} A_{oa} & B_{oa} \\ \hline C_{oa} & D_{oa} \end{array}\right] = \left[\begin{array}{cc|c} A_{ow} & B_{ow}C & B_{ow}D \\ 0 & A & B \\ \hline C_{ow} & D_{ow}C & D_{ow}D \end{array}\right].$$

Let the Gramians P_{ia} and Q_{ia}, representing weighted input-augmented controllability and weighted output-augmented observability Gramians, respectively, be given as follows:

$$P_{ia} = \begin{bmatrix} P_E & P_{12} \\ P_{12}^T & P_V \end{bmatrix},$$
$$Q_{oa} = \begin{bmatrix} Q_W & Q_{12}^T \\ Q_{12} & Q_E \end{bmatrix}.$$

These Gramian matrices P_{ia} and Q_{ia} satisfy the following Lyapunov equations:

$$A_{ia}P_{ia}A_{ia}^T - P_{ia} + B_{ia}B_{ia}^T = 0, \tag{8}$$
$$A_{oa}^T Q_{oa}A_{oa} - Q_{oa} + C_{oa}^T C_{oa} = 0. \tag{9}$$

Furthermore, P_E and Q_E represent the original system's input controllability and output observability Gramians, respectively. P_V and Q_W denote input-weighting controllability and output-weighting observability Gramians, respectively. Similarly, P_{12} is the controllability Gramian, and Q_{12} is the observability Gramian based on the number of inputs and outputs of input weighting and output weighting realizations, respectively.

2) ENNS MOR FRAMEWORK

To tackle MOR tasks efficiently, Enns developed a framework based on the idea of system augmentation. This method increases the computing efficiency of model reduction through the judicious use of augmented systems. By adding new states to the original system's state-space representation, Enns's methodology allows for a more comprehensive understanding of the system's dynamics. By adding new states to the system, we can better record crucial data, which speeds up the MOR process while methodically retaining important system properties. Enns's framework can derive ROMs while maintaining a balanced realization by deftly managing the augmented system [19].

By truncating the 1^{st} and 4^{th} blocks of (8) and (9), respectively, the resulting Lyapunov equations are as follows:

$$AP_EA^T - P_E + X_E = 0, \tag{10}$$
$$A^T Q_E A - Q_E + Y_E = 0. \tag{11}$$

Here, X_E and Y_E are defined as:

$$X_E = B_E B_E^T = BC_{iw}P_{12}^T A^T + AP_{12}C_{iw}^T B^T + BC_{iw}P_V C_{iw}^T B^T + BD_{iw}D_{iw}^T B^T, \tag{12}$$
$$Y_E = C_E^T C_E = C^T B_{ow}^T Q_{12}^T A + A^T Q_{12}B_{ow}C + C^T B_{ow}^T Q_W CB_{ow} + C^T D_{ow}^T D_{ow}C. \tag{13}$$

Applying eigenvalue decomposition on X_E and Y_E, we obtain:

$$X_E = U_E \text{diag}\left[S_{E_1}, S_{E_2}\right] U_E^T = U_E S_E U_E^T, \tag{14}$$
$$B_E = U_E \text{diag}\left[S_{E_1}^{1/2}, S_{E_2}^{1/2}\right] = U_E S_E^{1/2}, \tag{15}$$
$$Y_E = V_E \text{diag}\left[R_{E_1}, R_{E_2}\right] V_E^T = V_E R_E V_E^T, \tag{16}$$
$$C_E = \text{diag}\left[R_{E_1}^{1/2}, R_{E_2}^{1/2}\right] V_E^T = R_E^{1/2} V_E^T, \tag{17}$$

where $S_{E_1}, S_{E_2}, R_{E_1}$, and R_{E_2} are diagonal matrices containing positive and negative eigenvalues.

The transformation matrix T_E can be obtained as:

$$T_E^T Q_E T_E = T_E^{-1} P_E T_E^{-T} = \text{diag}[\zeta_1, \zeta_2, \zeta_3, \cdots, \zeta_n],$$

where $\zeta_j \geq \zeta_{j+1}$, $j = 1, 2, 3, \ldots, n-1$ and $\zeta_r > \zeta_{r+1}$. The transformation matrix T_E transforms the original stable large-scale system realization into a balanced realization. The ROM $H_{tr}[z] = C_{tr}[zI - A_{tr}]^{-1}B_{tr} + D_{tr}$ is acquired by partitioning the transformed realization in a similar way as in (4)-(5).

Remark 9: The input/output corresponding matrices X_E and Y_E may be indefinite, potentially impacting the stability of ROMs [19]. Furthermore, in certain frequency weighted realizations [35], the realization $\{A, B_E, C_E, D\}$ may not be necessarily minimal [35].

Remark 10: Enns's approach, with its frequency-weighted focus, will struggle to capture system dynamics adequately. There are worries regarding the stability and reliability of the resultant ROMs due to the uncertainty introduced by using indefinite matrices X_E and Y_E. Equally problematic for the ROM's precision is the possibility that the assumption of minimality in particular frequency weights won't hold up in actual practice [22].

Remark 11: Enns's MOR method maximizes efficiency for certain applications by focusing on frequency weighted Gramians [19]. Professionals should be aware of its apparent computing prowess but that it solely considers frequency weights. Applications necessitating complex frequency-interval insights are outside the scope of Enns's technique, notwithstanding its success in related tasks (i.e., frequency-interval Gramians). An approach that puts computing

economy ahead of exhaustive frequency-interval dynamics in certain cases [24], [26].

B. LIMITED-INTERVAL MOR PROBLEM

The WZ [21] offered pioneer frequency-limited framework built around discrete-time 1-D systems. Gramians are evaluated for the particular frequency intervals. These Gramian matrices P_J and Q_J for the particular frequency intervals are defined as:

$$P_J = P[\omega_2] - P[\omega_1], Q_J = Q[\omega_2] - Q[\omega_1],$$

where these Gramians be given as:

$$P_J[\omega] = \frac{1}{2\pi}\int_{\delta\omega}[e^{j\omega}I - A]^{-1}B_J B_J^T[e^{-j\omega}I - A^T]^{-1}d\omega,$$
$$Q_J[\omega] = \frac{1}{2\pi}\int_{\delta\omega}[e^{-j\omega}I - A^T]^{-1}C_J^T C_J[e^{j\omega}I - A]^{-1}d\omega,$$

where $\delta\omega = [\omega_1, \omega_2]$. These Gramians P_J and Q_J satisfy the following set of Lyapunov equation:

$$AP_JA^T - P_J + X_J = 0, \tag{18}$$
$$A^TQ_JA - Q_J + Y_J = 0, \tag{19}$$

where X_J and Y_J, $X_J = B_JB_J^T = (F[\omega_2] - F[\omega_1])BB^T + BB^T(F^*[\omega_2] - F^*[\omega_1])$ is the input corresponding matrix and $Y_J = C_J^TC_J = (F[\omega_2] - F[\omega_1])C^TC + C^TC(F^*[\omega_2] - F^*[\omega_1])$ is the output corresponding matrix attained in the particular frequency intervals $\delta\omega = [\omega_1, \omega_2]$, $F[\omega] = -\frac{\omega_2-\omega_1}{4\pi}I + \frac{1}{2\pi}\int_{\delta\omega}[e^{j\omega}I - A_*]^{-1}d\omega$ and $F^*[\omega]$ denote the conjugate transpose of the matrix $F[\omega]$. The following is obtained using the eigenvalues decomposition of X_J and Y_J.

$$X_J = U_J diag[S_{J_1}, S_{J_2}]U_J^T$$
$$\Longrightarrow B_J = U_J diag[S_{J_1}^{1/2}, S_{J_2}^{1/2}] = U_J S_J{}^{1/2},$$
$$Y_J = V_J diag[R_{J_1}, R_{J_2}]V_J^T$$
$$\Longrightarrow C_J = V_J diag[R_{J_1}^{1/2}, R_{J_2}^{1/2}] = R_J{}^{1/2}V_J^T,$$

where

$$S_{J_1} = diag[s_1, s_2, \ldots, s_{k_J}], S_{J_2} = diag[s_{k_J+1}, s_{k_J+2}, \ldots, s_n],$$
$$R_{J_1} = diag[r_1, r_1, \ldots, r_{p_J}], R_{J_2} = diag[r_{p_J+1}, r_{p_J+2}, \ldots, r_n],$$

S_{J_1} and R_{J_1} include (k_J) and (p_J) positive part of eigenvalues, respectively; in a similar manner, S_{J_2} and R_{J_2} include $(n-k_J)$ and $(n-p_J)$ negative part of eigenvalues, respectively.

Let T_J be the transformation matrix as:

$$T_J^TQ_JT_J = T_J^{-1}P_JT_J^{-T} = \text{diag}[\zeta_1, \zeta_2, \zeta_3, \cdots, \zeta_n],$$

where $\zeta_j \geq \zeta_{j+1}$, $j = 1, 2, 3, \ldots, n-1$ and $\zeta_r > \zeta_{r+1}$. The transformation matrix T_J transforms the original stable large-scale system realization into a balanced realization. The ROM $H_{tr}[z] = C_{tr}[zI - A_{tr}]^{-1}B_{tr} + D_{tr}$ is acquired by partitioning the transformed realization in a similar way as in (4)-(5).

Remark 12: For the particular frequency-range $\delta\omega = [-\pi, \pi]$, $lim_{\delta\omega\mapsto[-\pi,\pi]}\ P_{BT}[\delta\omega] = P_{BT} = P_J$, $lim_{\delta\omega\mapsto[-\pi,\pi]}\ Q_{BT}[\delta\omega] = Q_{BT} = Q_J$, where $P_{BT}[\delta\omega]$ and $Q_{BT}[\delta\omega]$ are acquired by employing Parseval's relationship [20], the ROM acquired by employing WZ [21] and BT [15] are same.

Remark 13: X_J and Y_J can be acquired for multiple frequency ranges [35], [36], [37].

Remark 14: WZ [21] sometime yield indefinite X_J and Y_J; consequently, generate unstable ROMs [25], [26], [37].

V. MAIN RESULTS

Enns's MOR framework [19] presents prominent challenges. The method has a tendency to produce ROMs that may exhibit instability, emphasizing the necessity for careful consideration when applying this approach to systems where stability is of paramount importance. Similarly, WZ's [21] MOR approach encounters a comparable limitation by primarily focusing on a restricted frequency spectrum. This characteristic could restrict its applicability in scenarios where a comprehensive understanding of the system's behavior across certain frequency-intervals is essential.

The instability issue in ROMs obtained using [19], [21] (i.e., both weighted and limited intervals scenarios) stems from the potential indefiniteness of matrices $X_{ind} \in \{X_E, X_J\} = \{B_EB_E^T, B_JB_J^T\} = \{[U_E\text{diag}\{S_{E_1}, S_{E_2}\}U_E^T], [U_J\text{diag}\{S_{J_1}, S_{J_2}\}U_J^T]\}$ and $Y_{ind} \in \{Y_E, Y_J\} = \{C_EC_E^T, C_J, C_J^T\} = \{[V_E\text{diag}\{R_{E_1}, R_{E_2}\}\ V_E^T], [V_J\text{diag}\{R_{J_1}, R_{J_2}\}V_J^T]$; subsequently, $B_{ind} \in \{B_E, B_J\} = \{[U_E\text{diag}\{S_{E_1}^{1/2}, S_{E_2}^{1/2}\}], [U_J\text{diag}\{S_{J_1}^{1/2}, S_{J_2}^{1/2}\}]\}$ and $C_{ind} \in \{C_E, C_J\} = \{[\text{diag}\{R_{E_1}^{1/2}, R_{E_2}^{1/2}\}V_E^T], [\text{diag}\{R_{J_1}^{1/2}, R_{J_2}^{1/2}\}V_J^T]$. This indefiniteness of matrices occurs when $S_{E_2} < 0$, $S_{J_2} < 0$, $R_{E_2} < 0$ and $R_{J_2} < 0$, where $S_{E_1} = \text{diag}\{s_1, s_2, \ldots, s_{k_E}\}$, $S_{J_1} = \text{diag}\{s_1, s_2, \ldots, s_{k_J}\}$, $S_{E_2} = \text{diag}\{s_{k_E+1}, s_{k_E+2}, \ldots, s_n\}$, $S_{J_2} = \text{diag}\{s_{k_J+1}, s_{k_J+2}, \ldots, s_n\}$, $R_{E_1} = \text{diag}\{r_1, r_2, \ldots, r_{p_E}\}$, $R_{J_1} = \text{diag}\{r_1, r_2, \ldots, r_{p_J}\}$, $R_{E_2} = \text{diag}\{r_{p_E+1}, r_{p_E+2}, \ldots, r_n\}$ and $R_{J_2} = \text{diag}\{r_{p_J+1}, r_{p_J+2}, \ldots, r_n\}$. Although [36] provides a solution to this limitation, the introduced approximation error in the frequency response is significant for the specified frequency-interval.

To address these drawbacks, the proposed MOR technique aims to offer a more versatile and stable approach for model reduction tasks. This paper introduces a novel approach that not only provides low-frequency response truncation error and stable ROMs but also yields an *a priori* formulation for the error-bound.

Definition 1: The proposed frequency-weighted-limited stability-preserving balanced model order reduction (FWL-SP-BMOR) technique aims to overcome instability challenges observed in existing weighted Gramians. It focuses on generating stable ROMs with minimal truncation error within a specified frequency-weighted framework. The FWL-SP-BMOR method is defined by the controllability ($P_{def} \in \{P_{w-def}, P_{l-def}\}$) and the observability ($Q_{def} \in \{Q_{wdef}, Q_{ldef}\}$) involves the following Gramians:

$$AP_{def}A^T - P_{def} + X_{def} = 0, \tag{20}$$
$$A^TQ_{def}A - Q_{def} + Y_{def} = 0. \tag{21}$$

Here, $X_{def} \in \{X_{wdef}, X_{ldef}\} = \{[B_{wdef} B_{wdef}^T], [B_{ldef} B_{ldef}^T]\}$ and $Y_{def} \in \{Y_{wdef}, Y_{ldef}\} = \{[C_{wdef} C_{wdef}^T], [C_{ldef} C_{ldef}^T]\}$, with $B_{def} \in \{B_{wdef}, B_{ldef}\}$ and $C_{def} \in \{C_{wdef}, C_{ldef}\}$ being proposed input and output-associated matrices, respectively.

Problem 1: Despite advancements in frequency-weighted and -limited balanced MOR techniques, existing methods encounter challenges in maintaining stability and minimizing approximation errors, particularly within a frequency-weighted and -limited context. This paper introduces the FWL-SP-BMOR method, aiming to produce stable ROMs with enhanced accuracy in capturing system dynamics over specified frequency-weights. The problem can be mathematically formulated as follows:

Given a LTI system described by matrices $\{A, B_{ind}, C_{ind}\}$, find a ROM $\{\hat{A}_{tr}, \hat{B}_{tr}, \hat{C}_{tr}, \hat{D}_{tr}\}$ with significantly fewer states while preserving stability and minimizing the error between the original system transfer function $H[z]$ and the reduced model transfer function $H_{tr}[z]$ within a frequency-weighted and -limited framework.

A. PROPOSED FRAMEWORK

The proposed input and output associated matrices, B_{def} and C_{def}, respectively, are given as:

$$B_{def} = U_{def} \begin{bmatrix} S_{EJ_1}^{1/2} & 0 \\ 0 & S_{def_2}^{1/2} \end{bmatrix} = U_{def} S_{def}^{1/2}, \tag{22}$$

$$C_{def} = \begin{bmatrix} R_{EJ_1}^{1/2} & 0 \\ 0 & R_{def_2}^{1/2} \end{bmatrix} V_{def}^T = R_{def}^{1/2} V_{def}^T, \tag{23}$$

where, $S_{EJ_1} \in \{S_{E_1}, S_{J_1}\}$, $R_{EJ_1} \in \{R_{E_1}, R_{J_1}\}$; furthermore, S_{def_2} and R_{def_2} are defined conditionally based on the signs of certain parameters. These matrices are computed as follows:

$$S_{def_2} = \begin{cases} \left[\dfrac{S_{EJ_2} - (\sum_{i=k_{EJ}+1}^{n} s_i) I}{-s_n} \right]^{1/2} & \text{for } s_n < 0 \\ S_{EJ_2}^{1/2} & \text{for } s_n \geq 0, \end{cases}$$

$$R_{def_2} = \begin{cases} \left[\dfrac{R_{EJ_2} - (\sum_{i=p_{EJ}+1}^{n} r_i) I}{-r_n} \right]^{1/2} & \text{for } r_n < 0 \\ R_{EJ_2}^{1/2} & \text{for } r_n \geq 0. \end{cases}$$

Similarly, here $S_{EJ_2} \in \{S_{E_2}, S_{J_2}\}$, $R_{EJ_2} \in \{R_{E_2}, R_{J_2}\}$; furthermore, $k_{EJ} \in \{k_E, k_J\}$ and $p_{EJ} \in \{p_E, p_J\}$.

1) STRUCTURAL PROPERTIES

Lemma 1: The proposed input and output matrices, X_{def} and Y_{def}, respectively, exhibit certain structural properties based on the given conditions. Specifically, when $X_{ind} \geq 0$ and $Y_{ind} \geq 0$, it implies certain relationships between P_{ind}, P_{def}, Q_{ind}, and Q_{def}.

Corollary 1: Under the conditions $X_{ind} \geq 0$ and $Y_{ind} \geq 0$, the relationships $P_{def} > 0$ and $Q_{def} > 0$ hold. Additionally, the conditions imply $P_{ind} \leq P_{def}$ and $Q_{ind} \leq Q_{def}$. Furthermore, the Hankel Singular Values (HSV) satisfy $(\lambda_i[P_{ind} Q_{ind}])^{1/2} \leq (\lambda_i[P_{def} Q_{def}])^{1/2}$.

Remark 15: The conditions $X_E \geq 0$ and $Y_E \geq 0$ imply certain structural properties in the Gramians, ensuring $P_{def} > 0$ and $Q_{def} > 0$. The stability of the ROM is demonstrated by providing a minimum and stable realization $\{A, B_{def}, C_{def}\}$. Given the stability of unweighted balanced truncation, the ROM is also stable.

B. PROPOSED TRANSFORMATION

The transformation matrix T_s is obtained to diagonalize Q_{def} and P_{def}:

$$\begin{aligned} T_{def}^T Q_{def} T_{def} &= T_{def}^{-1} P_{def} T_{def}^{-T} \\ &= \text{diag}\{\hat{\psi}_1, \hat{\psi}_2, \hat{\psi}_3, \ldots, \hat{\psi}_n\}, \end{aligned} \tag{24}$$

where $\hat{\psi}_i \geq \hat{\psi}_{i+1}$ and $\hat{\psi}_r \geq \hat{\psi}_{r+1}$. The transformed realization, denoted as $\{\hat{A}, \hat{B}, \hat{C}, \hat{D}\}$, is partitioned as:

$$T_{def}^{-1} A T_{def} = \hat{A} = \begin{bmatrix} \hat{A}_{tr} & \hat{A}_{12} \\ \hat{A}_{21} & \hat{A}_{22} \end{bmatrix}, T_{def}^{-1} B = \hat{B} = \begin{bmatrix} \hat{B}_{tr} \\ \hat{B}_2 \end{bmatrix}, \tag{25}$$

$$C T_{def} = \hat{C} = \begin{bmatrix} \hat{C}_{tr} & \hat{C}_2 \end{bmatrix}, \quad D = \hat{D}_{tr}. \tag{26}$$

$$\hat{H}[z] = \hat{C}_{tr}[zI - \hat{A}_{tr}]^{-1} \hat{B}_{tr} + \hat{D}_{tr}, \tag{27}$$

Remark 16: It is imperative to ensure the non-singularity of the matrix T_{def}. This condition can be expressed as:

$$det(T_{def}) \neq 0$$

where $det(T_{def})$ denotes the determinant of the matrix T_{def}. Verifying the non-singularity of T_{def} is essential for ensuring the validity and numerical stability of the subsequent mathematical operations.

C. ERROR BOUND ANALYSIS

This section analyzes the error bounds associated with the ROM obtained through the proposed framework. The error bound, as shown in Theorem 1, is a crucial metric that quantifies the accuracy of the ROM in approximating the original system. We establish a theoretical foundation for the error bound and present a formula that offers insights into the relationship between the error and the system parameters.

Theorem 1: A Priori Error Bound Formulation Let's consider a dynamic system characterized by the input-associated matrix B_{def} and output-associated matrices C_{def}. The ranks are such that $rank\begin{bmatrix} B_{def} & B \end{bmatrix} = rank\begin{bmatrix} B_{def} \end{bmatrix}$ and $rank\begin{bmatrix} C_{def} \\ C \end{bmatrix} = rank\begin{bmatrix} C_{def} \end{bmatrix}$. Under the assumption of asymptotic stability in the LTI original system (1) and the stability and minimality of the ROM (2), the proposed framework establishes stringent error bounds:

1) The term $\|W_{ow}[z](H[z] - \hat{H}_{tr}[z])V_{iw}[z]\|_\infty$ is bounded by:

$$2\|W_{ow}[z]\|_\infty \|L_{def}\|_\infty \|K_{def}\|_\infty \|V_{iw}[z]\|_\infty \sum_{j=r+1}^{n} \hat{\psi}_j.$$

2) The expression $\|(H[z]-\hat{H}_{tr}[z])V_{iw}[z]\|_\infty$ *is bounded by*:

$$2\|K_{def}\|_\infty\|V_{iw}[z]\|_\infty \sum_{j=r+1}^{n} \hat{\psi}_j.$$

3) The norm $\|W_{ow}[z](H[z]-\hat{H}_{tr}[z])\|_\infty$ *is bounded by*:

$$2\|W_{ow}[z]\|_2\|L_{def}\|_\infty \sum_{j=r+1}^{n} \hat{\psi}_j.$$

Here, L_{def} *and* K_{def} *take distinct forms based on the system's characteristics*:

$$L_{def} = \begin{cases} CV_{def}R_{def}^{-1/2} & \text{if } r_n < 0 \text{ exists} \\ CV_{ind}R_{ind}^{-1/2} & \text{otherwise,} \end{cases}$$

$$K_{def} = \begin{cases} S_{def}^{-1/2}U_{def}^{T}B & \text{if } s_n < 0 \text{ exists} \\ S_{ind}^{-1/2}U_{ind}^{T}B & \text{otherwise} \end{cases}$$

Proof: In this demonstration, we establish the proof for part **(1)** of Theorem 1, while parts **(2)** and **(3)** emerge as specific instances of this derivation. The rank conditions for the modified input-associated and output-associated matrices, as per [36], are expressed as follows:

$$\text{rank}\begin{bmatrix}B_{def} & B\end{bmatrix} = \text{rank}\begin{bmatrix}B_{def}\end{bmatrix} \text{ and rank}\begin{bmatrix}C_{def} \\ C\end{bmatrix} = \text{rank}\begin{bmatrix}C_{def}\end{bmatrix}.$$

Consequently, the interrelation between $B = B_{def}K_{def}$ and $C = L_{def}C_{def}$ persists. Through meticulous partitioning,

$$B_{def} = \begin{bmatrix}B_{def_1} \\ B_{def_2}\end{bmatrix}, C_{def} = \begin{bmatrix}C_{def_1} & C_{def_2}\end{bmatrix},$$

and subsequent substitution of $\hat{B}_{tr} = B_{def_1}K_{def}$, $\hat{C}_{tr} = L_{def}C_{def_1}$, we derive the following expression:

$$\begin{aligned}
&\|W_{ow}[z](H[z]-\hat{H}_{tr}[z])V_{iw}[z]\|_\infty \\
&= \|W_{ow}[z](C[zI-A]^{-1}B - \hat{C}_{tr}[zI-\hat{A}_{tr}]^{-1}\hat{B}_{tr})V_{iw}[z]\|_\infty \\
&= \|W_{ow}[z](L_{def}\ C_{def}[zI-A]^{-1}B_{def}\ K_{def} \\
&\quad - L_{def}\ C_{def_1}[zI-\hat{A}_{tr}]^{-1}B_{def_1})\ K_{def}V_{iw}[z]\|_\infty \\
&\le \|W_{ow}[z]\|_\infty\|L_{def}\|_\infty\|(C_{def}[zI-A]^{-1}B_{def} \\
&\quad - C_{def_1}[zI-\hat{A}_{tr}]^{-1}B_{def_1}\|_\infty\|K_{def}\|_\infty\|V_{iw}[z]\|_\infty.
\end{aligned}$$

If $\{\hat{A}_{tr}, B_{def_1}, C_{def_1}\}$ represents the ROM, and $\{A, B_{def}, C_{def}\}$ symbolizes the transformed realization; then, in accordance with [15], the inequality

$$\|(C_{def}[zI-A]^{-1}B_{def} - C_{def_1}[zI-\hat{A}_{tr}]^{-1}B_{def_1})\|_\infty \le 2\sum_{j=r+1}^{n}\hat{\psi}_j$$

holds.

As a result,

$$\begin{aligned}
&\|W_{ow}[z](H[z]-\hat{H}_{tr}[z])V_{iw}[z]\|_\infty \\
&\quad \le 2\|W_{ow}[z]\|_\infty\|L_{def}\|\|K_{def}\|_\infty\|V_{iw}[z]\|_\infty \sum_{j=r+1}^{n}\hat{\psi}_j.
\end{aligned}$$

This concludes the proof of part **(1)** of Theorem 1. ■

Corollary 2: Under the condition of exclusive input weighting, the boundedness of the error term $\|(H[z]-\hat{H}_{tr}[z])V_{iw}[z]\|_\infty$ *is bounded by*:

$$\|(H[z]-\hat{H}_{tr}[z])V_{iw}[z]\|_\infty \le 2\|K_{def}\|_\infty\|V_{iw}[z]\|_\infty\sum_{j=r+1}^{n}\hat{\psi}_j.$$

Similarly, in the presence of exclusive output weighting, the error term $\|W_{ow}[z](H[z]-\hat{H}_{tr}[z])\|_\infty$ *is bounded by*:

$$\|W_{ow}[z](H[z]-\hat{H}_{tr}[z])\|_\infty \le 2\|W_{ow}[z]\|_\infty\|L_{def}\|_\infty\sum_{j=r+1}^{n}\hat{\psi}_j.$$

Corollary 3: In scenarios where there is no input weighting, and output weights are unity, the error bound for the frequency-limited case is bounded by:

$$\|W_{ow}[z](H[z]-\hat{H}_{tr}[z])V_{iw}[z]\|_\infty \le 2\sum_{j=r+1}^{n}\hat{\psi}_j.$$

Corollary 4: When $X_{ind} \ge 0$ *and* $Y_{ind} \ge 0$*, it implies* $P_{ind} = P_{def}$ *and* $Q_{ind} = Q_{def}$*. Furthermore,* $P_{ind} < P_{def}$ *and* $Q_{ind} < Q_{def}$*. Additionally, the relation holds true for HSV:* $(\lambda_i[P_{ind}Q_{ind}])^{1/2} \le (\lambda_i[P_{def}Q_{def}])^{1/2}$.

Remark 17: The established error bounds, derived from rigorous proofs and corollaries, emphasize the robustness and precision of the proposed FWL-SP-BMOR framework. These bounds provide a thorough understanding of the interrelations between the original system, the ROM, and the impact of various weighting strategies. This analytical foundation ensures the reliability and accuracy of the MOR process, which is crucial for applications demanding precision in real-time systems.

D. PROPOSED ALGORITHM

This section presents the algorithmic steps for computing frequency-weighted ROM using the proposed framework. The algorithm 1 leverages the Gramian matrices to achieve a ROM with improved efficiency and computational performance.

VI. NUMERICAL EXAMPLES

Within the domain of power systems, this study presents numerical illustrations featuring variable speed-dependent WT and phase-locked loop for explanatory purposes. These instances encompass flux, current and phase-locked loop models derived from DFIGs and phase-locked loop parameters articulated within the discrete-time framework of MIMO and SISO systems, respectively. The primary objective of these examples is to assess the effectiveness of the proposed methodology relative to the prevailing state-of-the-art frequency-weighted and limited interval MOR techniques employed in discrete-time systems. This comparative analysis aims to contribute valuable insights to the existing body of knowledge in the field.

Furthermore, the study delves into an in-depth discussion of the frequency response error value and error-bound values

Algorithm 1 Computation of ROMs

procedure computeROMs(*model_equations*, *input_matrices*, *output_matrices*)
  Input: Original system as given in (1)
  Output: ROM corresponding to the given original system (27)
  Main program:
  model_equations ← [Lyapunov equations as in (10)-(11)]
  input_matrices ← [Input matrix as in (12)]
  output_matrices ← [Output matrix as in (13)]
  for each *align* **in** *model_equations* **do**
    if is Definite(*align*) **then**
      transformation_matrix ← compute Transformation Matrix(*equation as in (18)*)
      if is Stable(*transformation_matrix*) **then**
        additional Step1(*transformation_matrix*) ▷ Find frequency weighted for Gramians
    else
      modified_equation ← modify Equation(*equations as in (20)-(21)*)
      input_matrix as in (22), *output_matrix as in (23)* ← compute Matrices(*modified_equation*)
      transformation_matrix as in (24) ← compute Transformation Matrix(*input_matrix*, *output_matrix*)
      if is Stable(*transformation_matrix*) **then**
        additional Step1(*transformation_matrix*) ▷ Find frequency weighted for Gramians
    balanced_realization as in (25)-(26) ← compute Balanced Realization(*transformation_matrix*)
    ROM ← compute ROM(*balanced_realization*)
    store Results(*ROM*)
    additional Step2(*ROM* $\hat{H}_{tr}(s)$ as in (27)) ▷ Minimize error $\|y_o(t)(y(t) - y_{tr}(t))y_i(t)\|_2$
procedure isDefinite(*align*)
  return check Definiteness(*align*)
function computeTransformationMatrix(*align*)
  matrix ← extract Matrix(*align*)
  transformation ← compute Transformation(*matrix*)
  return *transformation*
function modify Equation(*align*)
  modified_equation ← modify(*align*)
  return *modified_equation*
function compute Matrices(*modified_equation*)
  input_matrix ← extract Input Matrix(*modified_equation*)
  output_matrix ← extract Output Matrix(*modified_equation*)
  return *input_matrix*, *output_matrix*
function compute Transformation Matrix(*input_matrix*, *output_matrix*)
  transformation_matrix ← compute Transformation(*input_matrix*, *output_matrix*)
  return *transformation_matrix*
function compute Balanced Realization(*transformation_matrix*)
  balanced_realization ← compute Balanced Realization(*transformation_matrix*)
  return *balanced_realization*
function compute ROM(*balanced_realization*)
  ROM ← compute ROM(*balanced_realization*)
  return *ROM*
function store Results(*result*)
  store(*result*)

derived from the error tables (i.e., Tables 4 and 5). This comparative analysis sheds light on the relative accuracy and efficiency of each method in capturing system dynamics. Additionally, the investigation extends to the pole location tables (i.e., Tables 6 and 7), specifically exploring the pole placements resulting from frequency-weighted and frequency-limited MOR techniques. The comparison of these tables contributes further insights into the transient behaviour and stability characteristics of the system under different reduction methodologies.

Example 1: Consider the state-space representation of a sixth-order MIMO LTI stable model, specifically the current model [27]. The system matrices are given by:

$$A=\begin{bmatrix} 0.6270 & 0.7790 & 0 & 0 & -0.0002 & -0.0003 \\ -0.7790 & 0.6270 & 0 & 0 & 0.0003 & -0.0002 \\ 0 & 0 & 0.6270 & 0.7790 & 0.0002 & 0.0003 \\ 0 & 0 & -0.7790 & 0.6270 & -0.0003 & 0.0002 \\ -0.0001 & -0.0001 & 0 & 0 & 0.3203 & 0.3951 \\ 0.0001 & -0.0001 & 0 & 0 & -0.3951 & 0.3172 \end{bmatrix}$$

$$B = e^{-5}\begin{bmatrix} -0.2516 & -0.1209 & -0.0036 & -0.0022 \\ 0.1209 & -0.2516 & 0.0022 & -0.0036 \\ -0.0043 & 0.0022 & 0.0212 & 0.0106 \\ 0.0016 & 0.0036 & -0.0106 & 0.0212 \\ -0.5190 & -0.8790 & -0.5217 & -0.8834 \\ 0.8790 & -0.5120 & 0.8834 & -0.5146 \end{bmatrix}$$

$$C = \begin{bmatrix} 0 & 0 & 1 & 0 & 0 & 0 \\ 0 & 0 & 0 & 1 & 0 & 0 \end{bmatrix}$$

$$D = [0]_{2\times 4}$$

Now, let's consider the weighted input and output realization matrices, denoted as A_{iw}, B_{iw}, C_{iw}, and D_{iw}, tailored to match the dimensions of the original system matrices.

$$A_{iw}=\begin{bmatrix} 0.8270 & 0.9790 & 0 & 0 & -0.0005 & -0.0006 \\ -0.9790 & 0.8270 & 0 & 0 & 0.0006 & -0.0005 \\ 0 & 0 & 0.8270 & 0.9790 & 0.0005 & 0.0006 \\ 0 & 0 & -0.9790 & 0.8270 & -0.0006 & 0.0005 \\ -0.0002 & -0.0002 & 0 & 0 & 0.5203 & 0.5951 \\ 0.0002 & -0.0002 & 0 & 0 & -0.5951 & 0.5172 \end{bmatrix}$$

$$B_{iw} = e^{-4}\begin{bmatrix} -0.1516 & -0.1209 & -0.0036 & -0.0022 \\ 0.1209 & -0.1516 & 0.0022 & -0.0036 \\ -0.0043 & 0.0022 & 0.0312 & 0.0206 \\ 0.0016 & 0.0036 & -0.0206 & 0.0312 \\ -0.4190 & -0.6790 & -0.4217 & -0.6834 \\ 0.6790 & -0.4120 & 0.6834 & -0.4146 \end{bmatrix}$$

$$C_{iw} = \begin{bmatrix} 0.9 & 0.8 & 0.7 & 0.6 & 0.5 & 0.4 \\ 0.3 & 0.2 & 0.1 & 0.9 & 0.8 & 0.7 \end{bmatrix}$$

$$D_{iw} = \begin{bmatrix} 0.9 & 0.8 & 0.7 & 0.6 \\ 0.5 & 0.4 & 0.3 & 0.2 \end{bmatrix}$$

Similarly, we define matrices A_{ow}, B_{ow}, C_{ow}, and D_{ow} for the output weighting scenario, tailored to match the dimensions of the original system matrices.

TABLE 4. Approximate error $\|W_{ow}[z](H[z]-\hat{H}_{tr}[z])V_{iw}[z]\|_\infty$.

Examples	$\hat{H}_{tr}[z]$	Error Values						Error Bound				
		BT [15]	Enns [19]	CB [22]	GS [23]	SI [24]	Proposed	Enns [19]	CB [22]	GS [23]	SI [24]	Proposed
Example 1	1^{st}	19.88	17.87	21.79	14.91	9.94	27.85	32.01	24.78	29.82	21.79	14.91
	2^{nd}	17.87	14.91	16.78	13.92	11.93	20.80	23.03	17.87	19.88	16.78	13.92
	3^{rd}	11.93	9.04	10.04	8.03	5.02	14.85	13.91	11.93	13.04	10.94	8.03
	4^{th}	4.97	3.00	4.02	2.00	0.99	8.01	9.03	5.01	6.02	3.00	1.98
	5^{th}	2.98	1.98	2.00	0.99	0.50	4.97	5.98	2.98	3.98	1.98	0.99
Example 2	1^{st}	27.79	24.78	26.78	21.78	17.82	34.79	36.74	31.73	33.66	29.82	24.78
	2^{nd}	24.78	21.78	23.76	19.80	14.85	31.73	33.66	27.72	29.70	24.78	19.80
	3^{rd}	19.80	17.82	18.90	14.85	9.90	27.74	29.70	24.78	25.82	21.78	17.82
	4^{th}	9.90	7.92	8.98	7.02	4.95	14.85	17.82	11.88	13.02	9.90	7.92
	5^{th}	4.95	2.97	3.98	1.98	0.99	8.01	8.98	4.97	5.96	2.97	1.98
Example 3	1^{st}	10.34	13.39	15.45	9.78	4.27	20.17	28.10	31.89	26.80	28.87	18.44

$$A_{ow}=\begin{bmatrix} 0.6270 & 0.7790 & 0 & 0 & -0.0002 & -0.0003 \\ -0.7790 & 0.6270 & 0 & 0 & 0.0003 & -0.0002 \\ 0 & 0 & 0.6270 & 0.7790 & 0.0002 & 0.0003 \\ 0 & 0 & -0.7790 & 0.6270 & -0.0003 & 0.0002 \\ -0.0001 & -0.0001 & 0 & 0 & 0.3203 & 0.3951 \\ 0.0001 & -0.0001 & 0 & 0 & -0.3951 & 0.3172 \end{bmatrix}$$

$$B_{ow}=e^{-4}\begin{bmatrix} -0.0516 & -0.0209 & -0.0036 & -0.0022 \\ 0.0209 & -0.0516 & 0.0022 & -0.0036 \\ -0.0043 & 0.0022 & 0.0112 & 0.0106 \\ 0.0016 & 0.0036 & -0.0106 & 0.0112 \\ -0.2190 & -0.3790 & -0.2217 & -0.3834 \\ 0.3790 & -0.3120 & 0.3834 & -0.3146 \end{bmatrix}$$

$$C_{ow}=\begin{bmatrix} 0.1 & 0.2 & 1.3 & 0.4 & 0.5 & 0.6 \\ 0.7 & 0.8 & 0.9 & 1.0 & 1.1 & 1.2 \end{bmatrix}$$

$$D_{ow}=\begin{bmatrix} 0.1 & 0.2 & 0.3 & 0.4 \\ 0.5 & 0.6 & 0.7 & 0.8 \end{bmatrix}$$

with the predefined frequency-range $[\omega_1, \omega_2] = [0.48\pi, 0.57\pi]$ *rad/sec. Tables 4 and 5 offer a concise summary of the approximation error in the context of predefined weights (i,e.,* $\|W_{ow}[z](H[z]-\hat{H}_{tr}[z])V_{iw}[z]\|_\infty$*) and predefined limited intervals (i,e.,* $\|H[z]-\hat{H}_{tr}[z]\|_\infty$*), respectively. We compare the ROMs produced by our novel method to those produced by the models based on unweighted [15], weighted [19], [22], [23], [24] and limited interval scenarios [21], [24], [25], [26] to conclude its efficacy. The superior accuracy and efficiency of the proposed approximations allow it to outperform competing approaches. Tables 6 and 7 demonstrate the many commonalities between the suggested and the existing approaches based on weighted [19] and limited interval scenarios [21], respectively. For the first five orders, the pole positions at* $z = 1.2457$, $z = 1.0445 \pm 1.4558i$, $z = 2.1224, 1.4478 \pm 1.2254i$, $z = 1.4458 \pm 1.0445i, -1.7889 \pm 1.0225i$ *and* $z = 2.4127, 1.02445 \pm 1.7021i, 0.5541 \pm 0.4489i$*, for the weighted MOR [19] and, the pole positions at* $z = 1.6732$, $z = 1.5562 \pm 1.0445i$, $z = 1.5574, 1.4485 \pm 1.0781i$, $z = 2.1145 \pm 1.0071i, 2.4412 \pm 1.0114i$ *and* $z = 1.4550, 1.4452 \pm 1.3455i, 1.4588 \pm 1.1233i$*, for the limited interval MOR [21], indicate that the ROMs generated are unstable. To deal with this, the suggested method builds stable ROMs in the given weighted and limited interval realization with an approximation error comparable to the existing stability-preserving methods.*

Example 2: Given the state-space expressions of a sixth-order MIMO LTI stable model (flux model [27]), let the matrices for the original system be:

$$A=\begin{bmatrix} -0.9027 & -0.4303 & 0 & 0 & 0 & 0 \\ 0.4303 & -0.9027 & 0 & 0 & 0 & 0 \\ 0 & 0 & 1 & 0 & 0 & 0 \\ 0 & 0 & 0 & 1 & 0 & 0 \\ 0 & 0 & 0 & 0 & 0.9913 & 0 \\ 0 & 0 & 0 & 0 & 0 & 0.9913 \end{bmatrix}$$

$$B=\begin{bmatrix} -0.0014 & 0.0061 & 0 & 0 \\ -0.0061 & -0.0014 & 0 & 0 \\ 0 & 0 & 0.0314 & 0 \\ 0 & 0 & 0 & 0.0314 \\ 0 & 0 & 0 & 0 \\ 0 & 0 & 0 & 0 \end{bmatrix}$$

$$C=\begin{bmatrix} 0 & 0 & 0.0010 & 0 & -0.0041 & 0 \\ 0 & 0 & 0 & 0.0010 & 0 & -0.0041 \end{bmatrix}$$

$$D=\begin{bmatrix} 0 \end{bmatrix}_{2\times 4}$$

Now, considering the input-weighted and output-weighted realizations with the given weight matrices, we have:

$$A_{iw}=\begin{bmatrix} -0.5012 & -0.3187 & 0 & 0 & 0.2483 & 0.0839 \\ 0.0182 & -0.4116 & 0 & 0 & -0.6354 & -0.4993 \\ 0 & 0 & 0.8642 & 0 & 0.7349 & 0.0644 \\ 0 & 0 & 0 & 0.8168 & 0.2448 & 0.0765 \\ 0.7415 & 0.2419 & 0 & 0 & 0.1542 & 0.1156 \\ 0.0016 & -0.0245 & 0 & 0 & -0.0467 & -0.9502 \end{bmatrix}$$

$$B_{iw}=\begin{bmatrix} -0.0061 & 0.0014 & 0 & 0 \\ -0.0084 & 0.0051 & 0 & 0 \\ 0.0002 & 0.0006 & 0.0314 & 0 \\ 0.0076 & -0.0054 & 0 & 0.0314 \\ 0.0012 & -0.0073 & 0 & 0 \\ -0.0017 & 0.0096 & 0 & 0 \end{bmatrix}$$

TABLE 5. Approximate error $\|H[z] - \hat{H}_{tr}[z]\|_\infty$.

Example	$\hat{H}_{tr}[z]$	Error Values						Error Bound				
		BT [15]	WZ [21]	IG [25]	TI [26]	SI [24]	Proposed	WZ [21]	IG [25]	TI [26]	SI [24]	Proposed
Example 1	1^{st}	20.57	18.51	22.55	15.41	10.34	28.75	33.10	25.62	30.65	22.55	15.41
	2^{nd}	18.51	15.41	17.44	14.47	12.41	21.56	23.77	18.51	20.57	17.44	14.47
	3^{rd}	12.41	9.41	10.41	8.31	5.20	15.34	14.41	12.41	13.55	11.41	8.31
	4^{th}	5.18	3.12	4.17	2.08	1.03	8.38	9.44	5.23	6.32	3.12	2.05
	5^{th}	3.10	2.07	2.10	1.03	0.52	5.15	6.23	3.10	4.17	2.07	1.03
Example 2	1^{st}	28.71	25.62	27.62	22.60	18.39	35.84	37.99	32.78	34.63	30.80	25.62
	2^{nd}	25.62	22.60	24.57	20.54	15.34	32.78	34.63	28.57	30.54	25.62	20.54
	3^{rd}	20.54	18.39	19.55	15.34	10.24	28.78	30.54	25.62	26.67	22.60	18.39
	4^{th}	10.24	8.18	9.24	7.23	5.07	15.34	18.39	12.27	13.42	10.24	8.18
	5^{th}	5.11	3.08	4.12	2.06	1.03	8.67	9.74	5.41	6.50	3.24	2.14
Example 3	1^{st}	10.46	15.37	12.49	11.56	7.38	21.23	17.91	26.11	28.59	24.66	12.14

TABLE 6. ROMs' poles locations for frequency weighted MOR.

Examples	$\hat{H}_{tr}[z]$	Enns [19]	Proposed
Example 1	1^{st}	1.2457	-0.8778
	2^{nd}	$1.0445 \pm 1.4558i$	$-0.1227 \pm 0.4557i$
	3^{rd}	$2.1224, 1.4478 \pm 1.2254i$	$-0.4558, -0.7745 \pm 0.4458i$
	4^{th}	$1.4458 \pm 1.0445i, -1.7889 \pm 1.0225i$	$-0.1447 \pm 0.0254i, -0.0144 \pm 0.1889i$
	5^{th}	$2.4127, 1.02445 \pm 1.7021i, 0.5541 \pm 0.4489i$	$0.4457, 0.0114 \pm 0.1447i, 0.1445 \pm 0.1178i$
Example 2	1^{st}	1.7741	0.0117
	2^{nd}	$1.5574 \pm 1.5548i$	$0.1145 \pm 0.1449i$
	3^{rd}	$1.0547, 1.1778 \pm 1.1187i$	$0.0445, -0.0441 \pm 0.1778i$
	4^{th}	$2.0554 \pm 1.1148i, 1.0048 \pm 1.1227i$	$-0.7889 \pm 0.7998i, -0.0078 \pm 0.7441i$
	5^{th}	$1.7789, 2.1889 \pm 1.1450i, 2.7841 \pm 2.4674i$	$0.7811, -0.1124 \pm 0.7714i, -0.4117 \pm 0.2778i$
Example 3	1^{st}	1.4967	0.1214

TABLE 7. ROMs' poles locations frequency limited MOR.

Examples	$\hat{H}_{tr}[z]$	WZ [21]	Proposed
Example 1	1^{st}	1.6732	-0.1145
	2^{nd}	$1.5562 \pm 1.0445i$	$-0.0045 \pm 0.7714i$
	3^{rd}	$1.5574, 1.4485 \pm 1.0781i$	$0.4112, -0.2244 \pm 0.4470i$
	4^{th}	$2.1145 \pm 1.0071i, 2.4412 \pm 1.0114i$	$-0.0778 \pm 0.0778i, -0.2214 \pm 0.1445i$
	5^{th}	$1.4550, 1.4452 \pm 1.3455i, 1.4588 \pm 1.1233i$	$-0.1447, -0.1227 \pm 0.0079i, -0.1223 \pm 0.0778i$
Example 2	1^{st}	1.0013	0.4417
	2^{nd}	$1.2547 \pm 1.4588i$	$0.1124 \pm 0.0014i$
	3^{rd}	$2.0080, 0.1124 \pm 0.0077i$	$0.1147, -0.2247 \pm 0.7798i$
	4^{th}	$1.7889 \pm 1.2145i, 1.7889 \pm 2.1248i$	$0.4478 \pm 0.2241i, 0.1248 \pm 0.7889i$
	5^{th}	$3.8996, 1.4577 \pm 1.4558i, 1.5457 \pm 1.7889i$	$0.7719, 0.4412 \pm 0.7442i, 0.1124 \pm 0.4412i$
Example 3	1^{st}	1.3372	0.2261

$$C_{iw} = \begin{bmatrix} 0 & 0 & 0.0090 & 0 & -0.0026 & 0.0065 \\ 0 & 0 & 0 & 0.0077 & 0.0098 & -0.0001 \end{bmatrix}$$

$$D_{iw} = \begin{bmatrix} 0.0045 & 0.0032 & 0.0078 & 0.0011 \\ 0.0023 & 0.0007 & 0.0036 & 0.0041 \end{bmatrix}$$

Similarly, we define matrices A_{ow}, B_{ow}, C_{ow}, and D_{ow} for the output weighting scenario, tailored to match the dimensions of the original system matrices.

$$A_{ow} = \begin{bmatrix} -0.0987 & -0.0532 & 0 & 0 & 0.0123 & 0.0356 \\ 0.0321 & -0.0714 & 0 & 0 & -0.0432 & -0.0281 \\ 0 & 0 & 0.1342 & 0 & 0.1123 & 0.0176 \\ 0 & 0 & 0 & 0.0871 & 0.0332 & 0.0257 \\ 0.0245 & 0.0127 & 0 & 0 & 0.0654 & 0.0456 \\ 0.0012 & -0.0058 & 0 & 0 & -0.0067 & -0.1081 \end{bmatrix}$$

$$B_{ow} = \begin{bmatrix} -0.0032 & 0.0051 & 0 & 0 \\ -0.0014 & 0.0023 & 0 & 0 \\ 0.0008 & 0.0019 & 0.0056 & 0 \\ 0.0017 & -0.0025 & 0 & 0.0056 \\ 0.0043 & -0.0071 & 0 & 0 \\ -0.0021 & 0.0043 & 0 & 0 \end{bmatrix}$$

$$C_{ow} = \begin{bmatrix} 0.2458 & 0.1423 & 1.2345 & 0.6564 & 0.8732 & 0.4971 \\ 0.8732 & 0.4971 & 0.2458 & 0.1423 & 0.2345 & 0.6564 \end{bmatrix}$$

$$D_{ow} = \begin{bmatrix} 0.0031 & 0.0027 & 0.0066 & 0.0009 \\ 0.0016 & 0.0005 & 0.0024 & 0.0027 \end{bmatrix}$$

swith the predefined frequency-range $[\omega_1, \omega_2] = [0.11\pi, 0.17\pi]$ rad/sec. Tables 4 and 5 offer a concise summary of the approximation error in the context of predefined weights

TABLE 8. Comparison of the existing and proposed framework among un-weighted [15], weighted [19], [22], [23], [24], and limited interval [21], [24], [25], [26] MOR.

Frameworks	Concept Addressed	Category	Challenge	Pros	Cons
Frequency Un-Weighted MOR Approach					
BT [15]	ROMs achieved by eliminating insignificant state variables while preserving the essential dynamics	Entire frequency domain	Computational complexity	MOR for the complex dynamical structure and preserves stability	Practical systems are not addressed, and there is a large error
Frequency Weighted MOR Approaches					
Enns [19]	ROMs achieved by specifically identifying and retaining dominant system poles in the frequency domain	Frequency-weighted MOR	Computational complexity	MOR for the complex dynamical structure and operates on frequency-weighted Gramians	Practical systems are not addressed, and stability is not guaranteed
CB [22]	ROMs achieved by specifically ensuring positive/semi-positive definiteness by taking the norm of all singular values	Frequency weighted MOR	ROM's stability is preserved	MOR for the complex dynamical structure	Practical systems are not addressed, unnecessary change in all singular values led to a large error
GS [23]	ROMs achieved by truncating negative half all singular values to get positive/semi-positive definiteness	Frequency-weighted MOR	ROM's stability is preserved	MOR for the complex dynamical structure	Truncating negative values create a significant variation from the original system
SI [24]	ROMs achieved by accumulative sum negative eigenvalues to the negative diagonal to get positive/semi-positive definiteness	Frequency-weighted MOR	ROM's stability is preserved	MOR for the complex dynamical structure	Zeroing the effect of last eigenvalues, results in a significant deviation from the original system
Proposed	ROMs achieved by specifically identifying and retaining dominant system poles by ensuring stability of WTs based DFIG by employing frequency weights	Frequency-weighted and limited interval MOR	Computational complexity and stability is preserved	MOR is done for real-time practical system by incorporating frequency weights to improve computational efficiency for DFIG and preserves the ROM's stability with less error	Analysis for time domain weighted and limited interval MOR is not given
Frequency Limited-Interval MOR Approaches					
WZ [21]	ROMs achieved by specifically identifying and retaining dominant system poles in the frequency domain	Frequency-limited intervals	Computational complexity	MOR for the complex dynamical structure and operates on frequency-limited intervals Gramians	Practical systems are not addressed, and stability is not guaranteed
IG [25]	ROMs achieved by specifically ensuring positive/semi-positive definiteness by subtracting least negative eigenvalues with all eigenvalues	Frequency limited MOR	ROM's stability is preserved	MOR for the complex dynamical structure	Practical systems are not addressed, unnecessary change for already positive eigenvalues led to a large error
TI [26]	ROMs achieved by employing geometrical manipulation to all singular values to get positive/semi-positive definiteness	Frequency-limited MOR	ROM's stability is preserved	MOR for the complex dynamical structure	Introducing geometrical function introduced more complication in input/output associated matrices create a significant variation from the original system
SI [24]	ROMs achieved by accumulative sum negative eigenvalues to the negative diagonal to get positive/semi-positive definiteness	Frequency-limited MOR	ROM's stability is preserved	MOR for the complex dynamical structure	Zeroing the effect of last eigenvalues, results in a significant deviation from the original system
Proposed	ROMs achieved by specifically identifying and retaining dominant system poles by ensuring stability of WTs based DFIG by employing frequency limited intervals	Frequency-weighted and limited interval MOR	Computational complexity and stability is preserved	MOR is done for real-time practical system by incorporating frequency limited intervals to improve computational efficiency for DFIG and preserves the ROM's stability with less error	Analysis for time domain weighted and limited interval MOR is not given

(i,e., $\|W_{ow}[z](H[z]-\hat{H}_{tr}[z])V_{iw}[z]\|_\infty$) and predefined limited intervals (i,e., $\|H[z]-\hat{H}_{tr}[z]\|_\infty$), respectively. We compare the ROMs produced by our novel method to those produced by the models based on unweighted [15], weighted [19], [22], [23], [24] and limited interval scenarios [21], [24], [25], [26] to conclude its efficacy. The superior accuracy and efficiency of the proposed approximations allow it to outperform competing approaches. Tables 6 and 7 demonstrate the many commonalities between the suggested and the existing approaches based on weighted [19] and limited interval scenarios [21], respectively. For the first five orders, the pole positions at $z = 1.7741$, $z = 1.5574 \pm 1.5548i$, $z = 1.0547, 1.1778 \pm 1.1187i$, $z = 2.0554 \pm 1.1148i$, $1.0048 \pm 1.1227i$ and $z = 1.7789, 2.1889 \pm 1.1450i$, $2.7841 \pm 2.4674i$, for the weighted MOR [19] and, the pole positions at $z = 1.0013$, $z = 1.2547 \pm 1.4588i$, $z = 2.0080, 0.1124 \pm 0.0077i$, $z = 1.7889 \pm 1.2145i$, $1.7889 \pm 2.1248i$ and $z = 3.8996, 1.4577 \pm 1.4558i$, $1.5457 \pm 1.7889i$, for the limited interval MOR [21], indicate that the ROMs generated are unstable. To deal with this, the suggested method builds stable ROMs in the given weighted and limited interval realization with an approximation error comparable to the existing stability-preserving methods.

Example 3: Consider a 2^{nd} order phase locked-loop model as given in [38], with the following 2^{nd} order input/output weighting state-space form

$$\left[\begin{array}{c|c} A_{iw} & B_{iw} \\ \hline C_{iw} & D_{iw} \end{array}\right] = \left[\begin{array}{cc|c} -0.75 & 0 & -0.25 \\ 0 & -0.75 & -0.24 \\ \hline -0.24 & 0.45 & 0 \end{array}\right],$$

$$\left[\begin{array}{c|c} A_{ow} & B_{ow} \\ \hline C_{ow} & D_{ow} \end{array}\right] = \left[\begin{array}{cc|c} -0.75 & 0 & -0.25 \\ 0 & -0.75 & -0.24 \\ \hline -0.24 & 0.45 & 0 \end{array}\right]$$

with the predefined frequency-range $[\omega_1, \omega_2] = [0.19\pi, 0.29\pi]$ rad/sec. Tables 4 and 5 offer a concise summary of the approximation error in the context of predefined weights (i,e., $\|W_{ow}[z](H[z]-\hat{H}_{tr}[z])V_{iw}[z]\|_\infty$) and predefined limited intervals (i,e., $\|H[z]-\hat{H}_{tr}[z]\|_\infty$), respectively. We compare the ROMs produced by our novel method to those produced by the models based on unweighted [15], weighted [19], [22], [23], [24] and limited interval scenarios [21], [24], [25], [26] to conclude its efficacy. The superior accuracy and efficiency of the proposed approximations allow it to outperform competing approaches. Tables 6 and 7 demonstrate the many commonalities between the suggested and the existing approaches based on weighted [19] and limited interval scenarios [21], respectively. For the first orders, the pole position at $z = 1.4967$, for the weighted MOR [19] and, the pole position at $z = 1.3372$, for the limited interval MOR [21], indicate that the ROMs generated are unstable. To deal with this, the suggested method builds stable ROMs in the given weighted and limited interval realization with an approximation error comparable to the existing stability-preserving methods.

ANALYSIS & DISCUSSION

As shown in Table 8, the proposed methodology considerably beats out the existing approaches that use frequency-weighted and constrained intervals, including the empirical evaluation. Since the empirical data has been thoroughly examined and discussed, the proposed methodology is compared in Tables 4 and 5 to alternative solutions that use frequency-unweighted values [15], frequency-weighted values [19], [22], [23], [24], and frequency-limited intervals [21], [24], [25], [26]. By outperforming existing methods in terms of approximation error reduction, the proposed methodology clearly demonstrates its dominance.

Derivation of ROMs across different orders is inherently unstable, as shown in Tables 6 and 7 (first through fifth). These results are compared to approaches suggested by [19] and [21], starting with initial stable flux and continuing with current models. The proposed methodology, on the other hand, is superior since it produces stable ROMs that are reinforced with error bounds, which improve accuracy and stability. The exact results in Tables 4 and 5 highlight the fact that the suggested methodology outperforms current state-of-the-art MOR strategies.

From the perspective of accuracy and reliability, as well as the amount of margin for error in the proposed method, the outcomes point to themselves. This illuminates the intricate role of order reduction in wind turbine model formulations.

VII. CONCLUSION

This research aims to analyze state-space systems in the discrete-time domain and assess their effectiveness in simplification using the proposed frequency-weighted and limited interval Gramian framework for model order reduction. Wind turbines, which may operate at varying speeds, are a prime illustration of this phenomenon. The simulation results demonstrate that the proposed method may efficiently and steadily reduce-order models. The approximation error that is produced by the proposed method is greatly reduced, which indicates that it works significantly better than existing stability-preserving model reduction techniques. One particularly remarkable aspect is the fact that this method provides analytical estimates for the bounds of errors. As a result, the operational efficiency and robustness of these reduced models have improved. Not only are these findings significant to academics who are actively engaged in the continual refinement of MOR techniques that are tailored to the complex dynamics of WTs, but the practical ramifications of these findings extend their importance to researchers as well. The innovative contributions made by this research pave the way for the development of the most advanced MOR for WTs, which will ultimately be of service to the larger field of renewable energy systems. Since the proposed approach only applicable for the frequency limited and weighted scenario; however, further research is necessary in case of time limited and weighted Gramians.

VIII. RECOMMENDATIONS AND FUTURE STUDIES

When it comes to the application of MOR approaches to WTs, the insights that were gathered from this research provide essential directions for further technical improvement. Researchers working on the topic are strongly encouraged to take into consideration the following suggestions and potential directions for further research:

1) **Application of Time-Constrained Gramians:** Particularly in the context of WT generators like DFIG and PMSG, the application of frequency-constrained Gramians holds a great deal of promise for MOR methods. This is especially true when it comes to the applications of these Gramians. In the event that additional research and optimization of this approach is carried out with the utilization of time-constrained Gramians, it is likely that enhanced reduction models for such systems can be established.
2) **Addressing Uncertainty and Disturbances:** Given the real-world unpredictability and uncertainties that are connected with renewable energy sources, the development of MOR methods that properly account for uncertainty and disturbances is a serious topic that needs to be addressed. If research is conducted using this approach, it may result in reduced models for WTs that are more robust and dependable.
3) **Advanced Optimization Techniques:** In order to contribute to the improvement of reduced models that may be used in WT applications, it can be helpful to make use of more advanced optimization techniques. Notable instances of these techniques are metaheuristic algorithms and evolutionary approaches. The most efficient configurations and parameter values can be determined with the assistance of these methods, which can be applied to be of expertise.
4) **Integration of Machine Learning:** Machine learning and machine learning together constitute one of the most promising new horizons in the field of artificial intelligence. Including machine learning techniques for model reduction, parameter adjustment, and data-driven modeling makes it possible to generate reduced-order models that are very efficient and accurate. This is achievable through the utilization of these techniques. This is especially relevant when taking WTs into consideration.
5) **Renewable Energy System Optimization:** In the realm of renewable energy systems, the optimization of models is an area that encompasses multiple disciplines. Researchers are strongly urged to investigate holistic approaches that take into account not just the individual components, such as WTs, but also their incorporation into broader renewable energy systems, such as microgrids and smart grids.

ACKNOWLEDGMENT

The authors would like to express their sincere gratitude to the following institutions for the significant contributions and support they have provided during this research endeavor. The Military College of Signals, National University of Sciences and Technology, Islamabad, Pakistan, is very much appreciated. In addition, highlighted is the collaboration with Sunway University, Malaysia.

(Muhammad Latif, Hira Ambreen, and Muhammad Imran contributed equally to this work.)

CONFLICT OF INTEREST STATEMENT

The authors declare that they have no conflict of interest regarding the publication of this article.

REFERENCES

[1] M. A. Syed, O. Siddiqui, M. Kazerani, and M. Khalid, "Analysis and modeling of direct ammonia fuel cells for solar and wind power leveling in smart grid applications," *IEEE Access*, vol. 12, pp. 46512–46523, 2024.

[2] F. Z. Abideen, H. A. Khalid, M. S. Khan, H. Rehman, and A. Hasan, "Direct model predictive control of fuel cell and ultra-capacitor based hybrid electric vehicle," *IEEE Access*, vol. 12, pp. 46512–46523, 2024.

[3] S. Mouassa, A. Alateeq, A. Alassaf, R. Bayindir, I. Alsaleh, and F. Jurado, "Optimal power flow analysis with renewable energy resource uncertainty using dwarf mongoose optimizer: Case of ADRAR isolated electrical network," *IEEE Access*, vol. 12, pp. 10202–10218, 2024.

[4] F. Stadtmann, A. Rasheed, T. Kvamsdal, K. A. Johannessen, O. San, K. Kölle, J. O. Tande, I. Barstad, A. Benhamou, and T. Brathaug, "Digital twins in wind energy: Emerging technologies and industry-informed future directions," *IEEE Access*, vol. 11, pp. 110762–110795, 2023.

[5] H. Chojaa, A. Derouich, O. Zamzoum, S. Mahfoud, M. Taoussi, H. Albalawi, H. Benbouhenni, and M. I. Mosaad, "A novel DPC approach for DFIG-based variable speed wind power systems using DSpace," *IEEE Access*, vol. 11, pp. 9493–9510, 2023.

[6] C. M. Emeghara, S. M. Mahajan, and A. Arzani, "Direct power control of a surface-mounted permanent magnet synchronous generator wind turbine for offshore applications," *IEEE Access*, vol. 11, pp. 62409–62423, 2023.

[7] N. Ullah, I. Sami, Md. S. Chowdhury, K. Techato, and H. I. Alkhammash, "Artificial intelligence integrated fractional order control of doubly fed induction generator-based wind energy system," *IEEE Access*, vol. 9, pp. 5734–5748, 2021.

[8] O. P. Mahela, N. Gupta, M. Khosravy, and N. Patel, "Comprehensive overview of low voltage ride through methods of grid integrated wind generator," *IEEE Access*, vol. 7, pp. 99299–99326, 2019.

[9] I. H. Panhwar, K. Ahmed, M. Seyedmahmoudian, A. Stojcevski, B. Horan, S. Mekhilef, A. Aslam, and M. Asghar, "Mitigating power fluctuations for energy storage in wind energy conversion system using supercapacitors," *IEEE Access*, vol. 8, pp. 189747–189760, 2020.

[10] B. Asad, T. Vaimann, A. Belahcen, A. Kallaste, A. Rassolkin, H. Van Khang, P. S. Ghahfarokhi, M. U. Naseer, and M. N. Iqbal, "The modeling and investigation of slot skews and supply imbalance on the development of principal slotting harmonics in squirrel cage induction machines," *IEEE Access*, vol. 9, pp. 165932–165946, 2021.

[11] A. S. Abdel-Khalik, M. S. Abdel-Majeed, and S. Ahmed, "Effect of winding configuration on six-phase induction machine parameters and performance," *IEEE Access*, vol. 8, pp. 223009–223020, 2020.

[12] J. Hashimoto, T. S. Ustun, M. Suzuki, S. Sugahara, M. Hasegawa, and K. Otani, "Advanced grid integration test platform for increased distributed renewable energy penetration in smart grids," *IEEE Access*, vol. 9, pp. 34040–34053, 2021.

[13] M. N. I. Sarkar, L. G. Meegahapola, and M. Datta, "Reactive power management in renewable rich power grids: A review of grid-codes, renewable generators, support devices, control strategies and optimization algorithms," *IEEE Access*, vol. 6, pp. 41458–41489, 2018.

[14] E.-T. Lee and H.-C. Eun, "Optimal sensor placement in reduced-order models using modal constraint conditions," *Sensors*, vol. 22, no. 2, p. 589, Jan. 2022.

[15] B. Moore, "Principal component analysis in linear systems: Controllability, observability, and model reduction," *IEEE Trans. Autom. Control*, vol. AC-26, no. 1, pp. 17–32, Feb. 1981.
[16] M. Imran and M. Imran, "Model order reduction framework for discrete-time systems with error bound via balanced structure," *Int. J. Syst. Sci.*, vol. 53, no. 14, pp. 3081–3094, Oct. 2022.
[17] M. Imran and M. Imran, "Transformation of two-dimensional model into two-dimensional decoupled model and decomposition into one-dimensional models," *Int. J. Syst. Sci.*, vol. 54, no. 3, pp. 491–503, 2023.
[18] M. Imran, "Transformation of two-dimensional Roesser model into two-dimensional decoupled model: Application to model reduction via balanced framework," *IEEE Trans. Syst., Man, Cybern., Syst.*, vol. 53, no. 9, pp. 5356–5368, Sep. 2023.
[19] D. F. Enns, "Model reduction with balanced realizations: An error bound and a frequency weighted generalization," in *Proc. 23rd IEEE Conf. Decis. Control*, Dec. 1984, pp. 127–132.
[20] A. V. Oppenheim and G. C. Verghese, *Signals, Systems & Inference*. London, U.K.: Pearson, 2017.
[21] D. Wang and A. Zilouchian, "Model reduction of discrete linear systems via frequency-domain balanced structure," *IEEE Trans. Circuits Syst. I, Fundam. Theory Appl.*, vol. 47, no. 6, pp. 830–837, Jun. 2000.
[22] K. Campbell, V. Sreeram, and G. Wang, "A frequency-weighted discrete system balanced truncation method and an error bound," in *Proc. Amer. Control Conf. (ACC)*, vol. 4, Jun. 2000, pp. 2403–2404.
[23] A. Ghafoor and V. Sreeram, "A survey/review of frequency-weighted balanced model reduction techniques," *J. Dyn. Syst., Meas., Control*, vol. 130, no. 6, pp. 061004-1–061004-16, 2008.
[24] S. Batool, M. Imran, and M. Imran, "Stability preserving model reduction technique for weighted and limited interval discrete-time systems with error bound," *IEEE Trans. Circuits Syst. II, Exp. Briefs*, vol. 68, no. 10, pp. 3281–3285, Oct. 2021.
[25] M. Imran and A. Ghafoor, "Stability preserving model reduction technique and error bounds using frequency-limited gramians for discrete-time systems," *IEEE Trans. Circuits Syst. II, Exp. Briefs*, vol. 61, no. 9, pp. 716–720, Sep. 2014.
[26] H. I. Toor, M. Imran, A. Ghafoor, D. Kumar, V. Sreeram, and A. Rauf, "Frequency limited model reduction techniques for discrete-time systems," *IEEE Trans. Circuits Syst. II, Exp. Briefs*, vol. 67, no. 2, pp. 345–349, Feb. 2020.
[27] C. E. Ugalde-Loo and J. B. Ekanayake, "State-space modelling of variable-speed wind turbines: A systematic approach," in *Proc. IEEE Int. Conf. Sustain. Energy Technol. (ICSET)*, Dec. 2010, pp. 1–6.
[28] S. Hlaing, "Basic concepts of doubly fed induction generator driven by wind energy conversion system," *Int. J. Sci. Eng. Technol. Res.*, vol. 3, nos. 15–2014, pp. 3242–3246, 2014.
[29] H. Holttinen and R. Hirvonen, "Power system requirements for wind power," in *Wind Power in Power Systems*, vol. 143. Hoboken, NJ, USA: Wiley, 2005, p. 167.
[30] A. R. Tiwari, A. J. Shewale, A. Gagangras, and N. M. Lokhande, "Comparison of various wind turbine generators," *Multidiscplinary J. Res. Eng. Technol.*, vol. 1, no. 2, pp. 129–135, 2014.
[31] Y. Kazachkov, J. W. Feltes, and R. Zavadil, "Modeling wind farms for power system stability studies," in *Proc. IEEE Power Eng. Soc. Gen. Meeting*, vol. 3, Jul. 2003, pp. 1526–1533.
[32] J. M. Rodríguez, J. L. Fernández, D. Beato, R. Iturbe, J. Usaola, P. Ledesma, and J. R. Wilhelmi, "Incidence on power system dynamics of high penetration of fixed speed and doubly fed wind energy systems: Study of the Spanish case," *IEEE Trans. Power Syst.*, vol. 17, no. 4, pp. 1089–1095, Nov. 2002.
[33] N. R. Ullah, A. Larsson, A. Petersson, and D. Karlsson, "Detailed modeling for large scale wind power installations—A real project case study," in *Proc. 3rd Int. Conf. Electr. Utility Deregulation Restructuring Power Technol.*, Apr. 2008, pp. 46–56.
[34] J. B. Ekanayake, L. Holdsworth, X. Wu, and N. Jenkins, "Dynamic modeling of doubly fed induction generator wind turbines," *IEEE Trans. Power Syst.*, vol. 18, no. 2, pp. 803–809, May 2003.
[35] M. Imran, A. Ghafoor, and M. Imran, "Frequency limited model reduction techniques with error bounds," *IEEE Trans. Circuits Syst. II, Exp. Briefs*, vol. 65, no. 1, pp. 86–90, Jan. 2018.
[36] S. Gugercin and A. C. Antoulas, "A survey of model reduction by balanced truncation and some new results," *Int. J. Control*, vol. 77, no. 8, pp. 748–766, May 2004.
[37] M. Imran, A. Ghafoor, and M. Imran, "Stability preserving model reduction technique for 1-D and 2-D systems with error bounds," *IEEE Trans. Circuits Syst. II, Exp. Briefs*, vol. 69, no. 3, pp. 1084–1088, Mar. 2022.
[38] S. Golestan and J. M. Guerrero, "Conventional synchronous reference frame phase-locked loop is an adaptive complex filter," *IEEE Trans. Ind. Electron.*, vol. 62, no. 3, pp. 1679–1682, Mar. 2015.

MUHAMMAD LATIF received the bachelor's and master's degrees in electrical engineering from the College of Electrical and Mechanical Engineering (CEME), National University of Sciences and Technology (NUST), Islamabad, Pakistan, in 2007 and 2016, respectively. He is currently pursuing the Ph.D. degree in electrical engineering with the Military College of Signals (MCS), NUST. He is immersed in intense research, regarding reduced-order controllers for large-scale power systems. He wants to use his knowledge in circumstances that require an understanding of more than one subject, so he's eager to research these undiscovered territories. His research interests include machine learning, robotics, and reducing model orders. A handful of his articles have appeared in prestigious journals of IEEE and Springer.

HIRA AMBREEN received the B.Sc. degree in electrical engineering from Sir Syed (Center for Advanced Studies) Institute of Technology, Islamabad, Pakistan, in 2024. She is conducting rigorous research on reduced-order controllers for large-scale power systems. Furthermore, she has done several research projects during her degree program, such as an IoT-based night vision line-tracking robot and a preserving stability algorithm for 2-D state space systems. Some of her most prestigious publications include conference proceedings and journals published by IEEE and Springer. Her expertise lies in model order reduction, robotics, and machine learning.

FARRUKH HASSAN (Graduate Student Member, IEEE) received the B.Sc. degree in computer science from the University of Peshawar, the M.I.T. degree from Gomal University, Dera Ismail Khan, Pakistan, the M.Sc. degree in computer science from Uppsala University, Sweden, in 2014, and the Ph.D. degree in information technology from Universiti Teknologi PETRONAS (UTP), Malaysia. From 2016 to 2019, he was a Faculty Member with Khushal Khan Khattak University, Karak, and the Abbottabad University of Science and Technology. His research interests include pattern recognition techniques involving seismic and acoustic emission signals using machine learning architecture.

MUHAMMAD IMRAN received the B.S. degree in electrical engineering from the University of Engineering and Technology (UET) Taxila, Pakistan, the degree in education, in 2014, and the M.S. and Ph.D. degrees in electrical engineering from the College of Electrical and Mechanical Engineering (CEME), National University of Sciences and Technology (NUST), Islamabad, Pakistan, in 2017 and 2022, respectively, with a focus on control systems (model/controller order reduction). He is currently pursuing postdoctoral research in nonlinear modeling and control design of UAVs with Guangdong CAS Cogniser Information Technology. He is an accomplished individual with substantial research knowledge across numerous fields. His numerous academic endeavors reflect his extensive viewpoint and commitment to examining the connections between many disciplines. He is a useful asset in robotics, unmanned aerial vehicles, and cyber security due to his distinctive viewpoint and wide range of skills. He is knowledgeable about both control and cyber-physical systems. Because of his extensive knowledge of modeling, simulation, and optimization, and his research experience in robotics and UAVs, he is qualified to create novel approaches for autonomous systems and address the intricate problems of cyber security in the context of robotics and UAV applications. His research interests include model order reduction, nonlinear control systems, fuzzy control, modeling, simulation, and optimization of dynamical systems, communication systems, signal processing, blockchain applications based on health care systems, cyber security, robotics, and unmanned aerial vehicles.

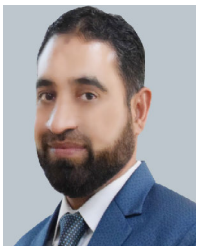

MUHAMMAD IMRAN received the bachelor's degree in electrical communication engineering from the School of Electrical Engineering and Computer Sciences (SEECS), National University of Sciences and Technology (NUST), Islamabad, Pakistan, in 2007, and the M.S. and Ph.D. degrees in electrical engineering from the Military College of Signals (MCS), NUST, in 2011 and 2014, respectively. So far, he has achieved remarkable success in his research, thanks to his outstanding education. As a result of his numerous scholarly articles and keynote speeches, he is highly esteemed by his colleagues. The NUST's Military College of Signals is his current place of employment. He was promoted to an Associate Professor for his significant contributions to the development of the academic unit and the institution. He is both a tenured Professor and the Associate Head of the Department. The breadth and depth of his interests reflect his extensive knowledge. His extensive body of work spans a wide variety of disciplines, including model/controller order reduction, stochastic modeling, communication, map-based mobile apps, unmanned autonomous vehicles, and biomedical algorithms. To better understand these problems and develop solutions, he conducts research across disciplines. No matter what field he's working in—education, research, or study—he never gives up until he succeeds.